J. Am. Chem. Soc. **1998,** *120,* 603−604

Carbon Nanotube Tips: High-Resolution Probes for Imaging Biological Systems

Stanislaus S. Wong,† James D. Harper,‡
Peter T. Lansbury, Jr.,*,‡ and Charles M. Lieber*,†

Department of Chemistry and Chemical Biology
Harvard University, 12 Oxford Street
Cambridge, Massachusetts 02138
Center for Neurologic Disease, Brigham and Women's
Hospital and Harvard Medical School
77 Avenue Louis Pasteur, Boston, Massachusetts 02115

Received November 3, 1997
Revised Manuscript Received December 10, 1997

Herein, we report the first atomic force microscopy (AFM) imaging studies with carbon nanotube tips that address their potential to improve lateral resolution and to probe biological systems. Multiwall carbon nanotubes (MWNTs) and single-wall carbon nanotubes (SWNTs) have been attached to the ends of single-crystal silicon cantilever tip assemblies and used to image amyloid β(1-40) derived protofibrils and fibrils by tapping mode AFM. Image analysis shows that the average resolution obtained with the nanotube tips is significantly better than that obtained with our best silicon tips and provides new insight into the structure and assembly mechanism of amyloid fibrils. The potential for imaging with molecular resolution using these tips is discussed.

The feature resolution obtained by AFM is determined in large part by the size and shape of the probe tip used for imaging.[1,2] Commercially available probes consist of microfabricated pyramids of Si or Si_3N_4 that have end radii of curvature as small as 10 nm but are often much larger.[2,3] These tips place significant constraints on potential lateral resolution, and furthermore, the pyramidal shape restricts the ability of these tips to access narrow and deep features. Small cone angle carbon protrusions with radii of 10−30 nm deposited on the ends of conventional tips significantly improve depth but not lateral resolution.[4] Recently, a potential breakthrough in probe technology was achieved by attaching MWNTs to the ends of Si tips.[5] In this work, the cylindrical geometry of the MWNT tips was exploited to image a deep grating with excellent fidelity, although potential improvements in lateral resolution were not investigated.

A typical scanning electron microscopy (SEM) image of a MWNT tip attached to a conventional single-crystal silicon cantilever tip assembly is shown in Figure 1.[5,6] This MWNT tip extends ca. 1.8 μm from the end of the pyramidal Si tip to which it is attached. The diameter of the major portion of the nanotube tip, 100 nm, is much larger than a single MWNT and corresponds to a bundle of tightly packed tubes.[7] The MWNT bundles attached to the Si probes have diameters of 75 ± 27 nm; attached SWNT bundles[8] typically are smaller with diameters of 45 ± 8 nm. The high aspect ratio nanotube tips have obvious advantages for probing deep crevices and steep features.[5] Additionally, it is

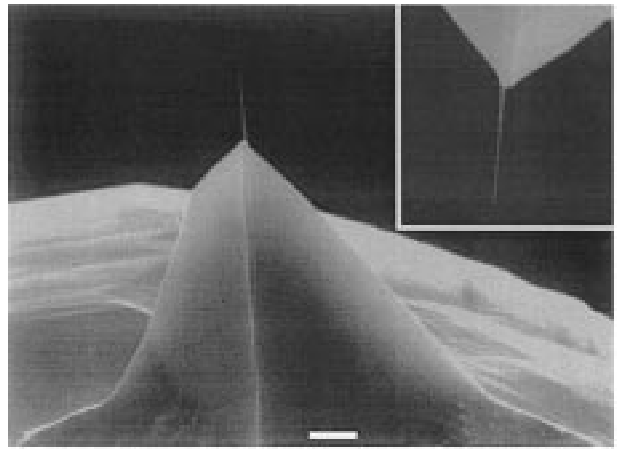

Figure 1. SEM image of a MWNT tip attached to a silicon cantilever tip assembly. The inset corresponds to a higher magnification view that highlights the nanotube. The orientation of the inset is rotated 180° relative to the main image. The white bar corresponds to 1 μm.

known that nanotubes elastically buckle above a critical force.[5,9] Buckling limits the maximum force applied to a sample,[10] which can prevent damage to delicate organic and biological samples, and at the same time makes the tips very robust.[9]

To explore the resolution of these tips and their applicability to high-resolution imaging of biological samples, we have investigated amyloid-β 1-40 (Aβ40) fibrils produced in vitro. Aβ fibrils are the primary constituent of the insoluble core of amyloid plaques that are characteristic of Alzheimer's disease.[11] Previous AFM studies have shown that Aβ initially forms protofibril structures[12,13] and subsequently larger fibrils;[12−14] branching of fibrils has also been observed.[13,14] A typical image[15] of an Aβ fibril obtained with a MWNT tip (Figure 2) shows higher resolution than observed in previous AFM studies of the fibrils. Key features include (1) a fibril Y-branch (left arrow) with the

† Harvard University.

‡ Brigham and Women's Hospital and Harvard Medical School.

(1) (a) Quate, C. F. *Surf. Sci.* **1994**, *299/300*, 980. (b) Rugar, D.; Hansma, P. *Phys. Today* **1990**, *43* (10), 23. (c) Noy, A.; Vezenov, D.; Lieber, C. M. *Annu. Rev. Mater. Sci.* **1997**, *27*, 381.

(2) (a) Hansma, H. G.; Hoh, J. H. *Annu. Rev. Biophys. Biomol. Struct.* **1994**, *23*, 115. (b) Bustamante, C.; Keller, D. *Phys. Today* **1995**, *48* (12), 32. (c) Shao, Z.; Yang, J. *Quart. Rev. Biophys.* **1995**, *28*, 195.

(3) Itoh, J.; Tohma, Y.; Kanemaru, S.; Shimizu, K. *J. Vac. Sci. Technol. B* **1995**, *13*, 331.

(4) (a) Keller, D. J.; Chih-Chung, C. *Surf. Sci.* **1992**, *268*, 333. (b) Zenhausern, F.; Adrian, M.; Heggeler-Bordier, B.; Ardizzoni, F.; Descouts, P. *J. Appl. Phys.* **1993**, *73*, 7232.

(5) Dai, H.; Hafner, J. H.; Rinzler, A. G.; Colbert, D. T.; Smalley, R. E. *Nature* **1996**, *384*, 147.

(6) MWNTs and SWNTs were prepared by arc discharge[7] and laser vaporization[8] methods, respectively. MWNT samples were purified by oxidation (700 °C, air) until ~2% of the original mass remained. SWNT samples were purified by sonication and filtration through 0.8 μm pore membranes. Nanotubes were attached to the pyramids of gold-coated Si cantilevers (FESP, (k = 1−5 N/m), Digital Instruments, Inc., Santa Barbara, CA) using an acrylic adhesive (adhesive carbon tape, Electron Microscopy Services, Fort Washington, PA) under the direct view of an optical microscope. The as-made nanotube tips are typically too long for high-resolution imaging and were shortened by applying a bias voltage between the tip and a sputtered Nb surface.

(7) Colbert, D. T.; Zhang, J.; McClure, S. M.; Nikolaev, P.; Chen, Z.; Hafner, J. H.; Owens, D. W.; Kotula, P. G.; Carter, C. B.; Weaver, J. H.; Rinzler, A. G.; Smalley, R. E. *Science* **1994**, *266*, 1218.

(8) Thess, A.; Lee, R.; Nikolaev, P.; Dai, H.; Petit, P.; Robert, J.; Xu, C.; Lee, Y. H.; Kim, S. G.; Rinzler, A. G.; Colbert, D. T.; Scuseria, G. E.; Tomanek, D.; Fischer, J. E.; Smalley, R. E. *Science* **1996**, *273*, 483.

(9) Wong, E. W.; Sheehan, P. E.; Lieber, C. M. *Science* **1997**, *277*, 1971.

(10) The buckling force, F_B, can be estimated from $F_B = \pi^2 EI/L^2$ where E is Young's modulus, I is the moment of inertia $\pi r^4/4$, and L is the length of the unsupported nanotube. For typical radii r, L and E = 1.2 T Pa,[9] the range of buckling forces will be 5−30 nN.

(11) (a) Lansbury, P. T. *Acc. Chem. Res.* **1996**, *29*, 317. (b) Selkoe, D. J. *Science* **1997**, *275*, 630.

(12) Harper, J. D.; Wong, S. S.; Lieber, C. M.; Lansbury, P. T. *Chem. Biol.* **1997**, *4*, 119.

(13) Harper, J. D.; Lieber, C. M.; Lansbury, P. T. *Chem. Biol.*, in press.

(14) Stine, W. B.; Snyder, S. W.; Ladror, U. S.; Wade, W. S.; Miller, M. F.; Perun, T. J.; Holzman, T. F.; Krafft, G. A. *J. Protein Chem.* **1996**, *15*, 193.

(15) All images were acquired with a Nanoscope III instrument (Digital Instruments, Santa Barbara, CA) under ambient conditions in tapping mode. All samples were prepared by depositing a 3−5 μL aliquot of Aβ40 solution on freshly cleaved mica surfaces and then rinsing twice with 50 μL of water.[12,13] Imaging parameters were optimized for individual tips; typical ranges for the FESP nanotube tips were (i) free RMS oscillation amplitude, 30−40 nm, (ii) setpoint voltage, 0.45−0.80 V, and (iii) scan rate, 0.25−1 Hz.

S0002-7863(97)03773-6 CCC: $15.00
Published on Web 01/08/1998

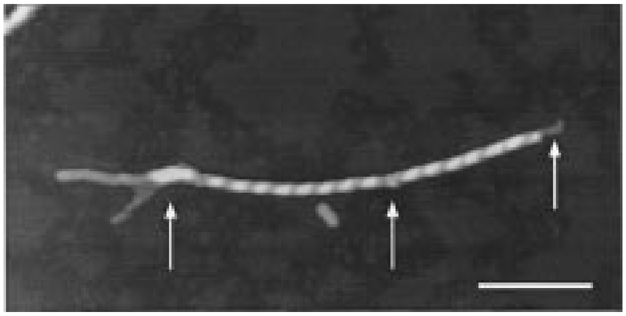

Figure 2. Typical AFM image of a type I[12] Aβ40 fibril acquired with a MWNT tip. The arrows highlight specific features discussed in the text. The white bar corresponds to 250 nm.

lower arm of the Y approximately one-half of the height of the major fibril body, (2) a defect in the periodic structure (middle arrow), and (3) a staggered fibril end (right arrow). A critical difference between the present data of the Y-branch and previous studies[14] is the decrease in size after branching. The Y-branch and staggered end are believed to correspond to active growth sites to which protofibrils add during fibril assembly[13] and are thus indicative of the potential of nanotube tips for unraveling the growth mechanism of Aβ fibrils. In addition, we find that the MWNT and SWNT tips are more robust and less prone to contamination than Si tips. Adhesion forces observed with our nanotube tips are also typically 2−5 times smaller than those found for our sharpest Si tips, thus enabling gentler imaging conditions.[16] Moreover, when the resolution of a nanotube tip deteriorates (e.g., due to contamination), the simple field evaporation process used to shorten the tip can regenerate an optimal tip.[6]

To quantify the resolution of the new nanotube tips, we have compared the diameters and the height variation along the periodic structures of fibrils and protofibrils with the corresponding values obtained with single-crystal Si tips. These results are summarized in Table 1. On average we find that the observed widths of the fibrils and protofibrils are 3−8 nm smaller for MWNT tips than those for our best Si tips,[17] confirming the qualitative interpretation of the images. This corresponds to a 12−30% increase in resolution. MWNT tips also generally exhibit a greater height variation along the fibril and protofibril axes than Si tips, presumably due to their high-aspect ratio. In addition, preliminary measurements made with SWNT[8] tips show that significantly higher lateral resolution is possible. Notably, we find a 10−15 nm reduction in the observed fibril diameter compared to Si tips and, thus, are approaching the limit of no tip-induced broadening of the fibril structure.

Table 1. Summary of Data Comparing the Resolution Obtained with Nanotube and Silicon Tips on Aβ40 Fibrils and Protofibrils

sample	tip	width at half-maximum (nm)[a]	depth between subunits (nm)[b]	tip radius (nm)[c]
type-1 fibril	MWNT	18.6 ± 2.2	3.2 ± 0.4	9.3
	SWNT	11.9 ± 0.7	2.7 ± 0.4	2.6
	Si-TESP	26.0 ± 0.9	2.7 ± 0.3	19.7
	Si-FESP	21.5 ± 1.8	2.5 ± 0.3	12.9
protofibril	MWNT	11.4 ± 0.4	1.1 ± 0.1	9.7
	Si-TESP	14.4 ± 0.3	0.6 ± 0.1	15.9
	Si-FESP	14.8 ± 1.7	0.7 ± 0.2	16.9

[a] The widths at half-maximum were determined from cross-sections taken perpendicular to the fibril and protofibril axes. [b] Maximum-to-minimum height variations determined from cross-sections taken along the periodic fibril/protofibril axes. [c] The effective tip radii were calculated[18] for diameters of the fibril and protofibril of 7.8 and 3.1 nm, respectively.[12] The fibril and protofibril heights measured with the nanotube and Si tips were consistent with these diameters.

The improvement in resolution is due primarily to a reduction in the effective tip radii when imaging with nanotube tips. We have calculated the effective nanotube and Si tip radii by using standard deconvolution methods[18] and compare these results in Table 1.[19] These data highlight the improvements achieved with the nanotube tips. In particular, the average MWNT tips exhibit radii of 9 nm compared with 13−20 nm for Si.[17] Even more impressive are the initial results obtained with SWNTs that show an average effective radius of only 3 nm. We believe that the use of SWNT tips is especially promising, since the observed radii are still substantially larger than the 0.5−0.7 nm radii of individual SWNTs;[8] i.e., sharper tips will be achievable if methods to expose individual tubes at the tip ends are developed. These studies demonstrate for the first time that significantly improved lateral resolution is attainable on biological samples using MWNT and SWNT probe tips. While further improvements in resolution will be needed in order to approach true molecular resolution imaging in air and in liquids, we believe that nanotube tips offer a rational pathway to do so in the future.

Acknowledgment. We thank D. Vezenov, A. Noy, A. Morales, P. Yang, H. Dai, J. Hafner, and J. Liu for helpful discussions. C.M.L. and P.T.L. acknowledge support of this work by the NIH National Institute on Aging (P01 AG14366), and S.S.W. acknowledges fellowship support from the Natural Sciences and Engineering Research Council of Canada.

JA9737735

(16) Lower adhesion forces enable smaller spring constant cantilevers to be used reliably in tapping mode without resorting to large drive amplitudes, and this can reduce sample deformation. The lower adhesion forces observed with the nanotube tips are believed to be due to a combination of the smaller tip radii and lower surface energy compared to those with Si tips.

(17) The values listed in Table 1 for nanotube tips are an average and have not been selected to highlight the best resolution tips. In contrast, the values listed for the Si tips correspond to our best tips. Significantly poorer resolution is often observed with blunt or contaminated Si tips. The specified nominal radii of our commercial Si tips are 5−10 nm, although the effective radii observed in our measurements are always ≥10 nm.

(18) Bustamante, C.; Keller, D.; Yang, G. *Curr. Opin. Struct. Biol.* **1993**, *3*, 363.

(19) Similar results were obtained from the analysis of images of 5 and 10 nm Au colloids (Ted Pella, Redding, CA) recorded using nanotube and Si tips. Au colloids have been used previously as an imaging standard: Vesenka, J.; Manne, S.; Giberson, R.; Marsh, T.; Henderson, E. *Biophys. J.* **1993**, *65*, 992.